Neuropharmacology 128 (2018) 388–400

Contents lists available at ScienceDirect

Neuropharmacology

journal homepage: www.elsevier.com/locate/neuropharm

Kainate receptor mediated presynaptic LTP in agranular insular cortex contributes to fear and anxiety in mice

Tian-Yao Shi [a, b, 1], Shu-Fang Feng [c, 1], Ming-Xiao Wei [a, b], Yan Huang [a, b], Gang Liu [a, b], Hai-Tao Wu [d], Yong-Xiang Zhang [a, b], Wen-Xia Zhou [a, b, *]

[a] Department of Neuroimmunopharmacology, Beijing Institute of Pharmacology and Toxicology, Beijing, China
[b] State Key Laboratory of Toxicology and Medical Countermeasures, Beijing, China
[c] Department of Poisoning and the Treatment, Affiliated Hospital to Academy of Military Medical Sciences (the 307 Hospital), Beijing, China
[d] Department of Neurobiology, Beijing Institute of Basic Medical Sciences, Beijing, 100850, China

ARTICLE INFO

Article history:
Received 2 May 2017
Received in revised form
24 October 2017
Accepted 28 October 2017

ABSTRACT

Anxiety disorders represent serious social problems worldwide. Recent neuroimaging studies have found that elevated activity and altered connectivity of the insular cortex might account for the negative emotional states in highly anxious individuals. However, the exact synaptic mechanisms of specific insular subregions have yet to be studied in detail. To assess the electrophysiological properties of agranular insular cortex (AIC) neurons, basic synaptic transmission was recorded and different protocols were used to induce presynaptic and postsynaptic long-term potentiation in mice with anxiety-related behaviors. The presynaptic membrane expression of kainate receptors (KARs) and pharmacologic manipulations were quantified to examine the role of Gluk1 subtype in anxiety-like behaviors. Fear conditioning occludes electrically induced postsynaptic-LTP in the AIC. Quantal analysis of LTP expression in this region revealed a significant presynaptic component reflected by an increase in the probability of transmitter release. A form of presynaptic-LTP that requires KARs has been characterized. Interestingly, a simple emotional anxiety stimulus resulted in selective occlusion of presynaptic-LTP, but not of postsynaptic-LTP. Finally, injecting GluK1-specific antagonists into the AIC reduced behavioral responses to fear or anxiety stimuli in the mouse. These findings suggest that activity-dependent synaptic plasticity takes place in the AIC due to exposure to fear or anxiety, and inhibiting the presynaptic KAR function may help to prevent or treat anxiety disorder.

1. Introduction

Most clinical anxiety disorders such as post-traumatic stress disorder (PTSD) are characterized by an exaggerated fear response or hyperarousal, which is believed to be reflected in the enhanced emotional salience processing (Shin and Liberzon, 2010; Peterson et al., 2014). Recent research indicates that a broader set of brain regions can influence the processing of salient stimuli (Seeley et al., 2007). Emerging evidence indicates that the insular cortex, an important part of the interoceptive system (Craig, 2002), is a key node of the salience network that generates subjective feelings of emotion (Uddin, 2015; Paulus and Stein, 2006; Craig, 2009). Based on functional neuroimaging findings, the insular cortex is reliably over-activated in many anxiety disorders (Etkin and Wager, 2007; Grupe and Nitschke, 2013), and it may contribute to the mediation of intense and persistent fear symptoms (Wendt et al., 2008). Surgical lesions or chemical inactivation of the insular cortex produces anxiolytic effects in humans (Terasawa et al., 2015) and animals (Alves et al., 2013). However, little is known about the reasons for aberrant salience processing, and the molecular and cellular basis of anxiety in the insular cortex. The insular cortex is divided into three major divisions based on granularity: granular, dysgranular, and agranular. Anatomical tracing studies indicate that the AIC serves as a crucial site of convergence to receive sensory perception (Saper, 1982) and has connections with limbic regions including the amygdala, thalamus, and medial prefrontal cortex (Shi and Cassell, 1998), thereby suggesting a critical role for this area in emotional processing. The present study was undertaken to

* Corresponding author. Department of Neuroimmunopharmacology, Beijing Institute of Pharmacology and Toxicology, Room 502, Building No.12, Taiping Rd.27, Haidian District, Beijing, 100850, China.
E-mail address: zhouwx@bmi.ac.cn (W.-X. Zhou).
[1] These authors contributed equally to this work, as co-first authors.

https://doi.org/10.1016/j.neuropharm.2017.10.037
0028-3908/

explore the contribution of AIC subregions in a rodent model of fear and anxiety disorder.

The most commonly used procedure for studying learned fear has been Pavlovian fear conditioning with neutral conditioned stimuli (CS) and aversive unconditioned stimuli (US) (LeDoux, 2000). Some anxiety patients exhibit increased conditional fear (LeDoux, 2012), and the acquisition of fear has been found to be mediated by LTP-like synaptic enhancements of several brain structures, such as the amygdala (Rogan et al., 1997), hippocampus (Nicoll and Schmitz, 2005), and prefrontal cortex (Gilmartin et al., 2014) in animal studies. Two major forms of LTP have been observed, depending on the degree of postsynaptic depolarization and presynaptic activity levels. Conventional theta burst-induced LTP, pairing-induced LTP, and spike timing-dependent LTP are expressed post-synaptically, or called postsynaptic LTP, which is based on activation of NMDA receptors (NMDARs) and regulation of post-synaptic AMPA receptor (AMPAR) trafficking into synapses (Rumpel et al., 2005; Bliss and Collingridge, 2013). Contrastingly, LTP in thalamic input to the amygdala is expressed pre-synaptically, or called presynaptic LTP due to an enhanced probability of neurotransmitter release mediated by KARs (Shin et al., 2010). Moreover, upon LTP induction in the anterior cingulate cortex after neuropathic pain, a pre-LTP and post-LTP of AMPAR-mediated responses coexist (Xu et al., 2008). However, whether these two forms of LTP coexist in the AIC during the salience processing of anxiety disorders remains unknown.

KARs, as important glutamate receptors, are now widely believed to play a crucial role in the control of synaptic transmissions in multiple brain areas (Lerma, 2003; Jane et al., 2009; Jaskolski et al., 2005; Nistico et al., 2011). The KAR family is composed of five different subunits (GluK1–5). GluK1-containing KARs are involved in the formation of LTP in hippocampus (Bortolotto et al., 1999) and amygdala (Shin et al., 2013) and are related to emotional disorders, such as anxiety (Wu et al., 2007) and fear (Ko et al., 2005). Previous studies have indicated that KARs mediate synaptic transmissions in the insular cortex of adult rodent models (Koga et al., 2012). In this study, we found that presynaptic and postsynaptic LTP mechanisms coexist in the AIC of rodent models during fear conditioning, and that presynaptic-LTP could be selectively occluded by anxiety. We also found that administering GluK1 antagonist in the AIC can erase presynaptic-LTP and reduce the potentiation of behavioral anxiety.

2. Materials and methods

2.1. Animals

Adult wild-type C57Bl6/6J male mice were used in the experiments. Mice were housed in a 12:12 h light and dark cycle (light-on between 8 a.m. and 8 p.m.) with food and water provided ad libitum. All mouse protocols were consistent with the National Institute of Health guidelines and were approved by the Animal Care and Use Committee of Beijing Institute of Pharmacology and Toxicology.

2.2. Brain slice preparations and electrophysiology

The rostrocaudal levels corresponded to 0.7–1.7 mm anterior insular cortex, relative to the bregma (Paxinos and Franklin, 2001). The mice were anesthetized with 2% halothane, and coronal brain slices (300 μm) containing the anterior insular cortex were cut at 4 °C with a vibratome in oxygenated artificial cerebrospinal fluid (ACSF), containing 124 mM NaCl, 2 mM KCl, 26 mM $NaHCO_3$, 2 mM $CaCl_2$, 2 mM $MgSO_4$, 1 mM NaH_2PO_4, and 10 mM D-glucose (pH 7.4). For electrophysiological experiments, the brain slices were transferred to a submerged recovery chamber with oxygenated ACSF at room temperature. For biochemical experiments, the slices were slowly brought to a final temperature of 30 °C in ACSF aerated with 95% O_2/5% CO_2 and incubated for 1 h. The slices were then exposed to different compounds for the indicated times, and the anterior insular cortex regions were micro-dissected and snap-frozen over dry ice.

Experiments were performed in a recording chamber on a microscope stage equipped with infrared differential interference contrast optics for visualization. For recordings in the AIC, the excitatory postsynaptic currents (EPSCs) were recorded from layer II/III neurons with an Axon 700B amplifier (Molecular Devices, USA), and the stimulations were delivered by a bipolar tungsten electrode placed in layer V/VI of the AIC. AMPAR-mediated EPSCs were induced by repetitive stimulations at 0.02 Hz, and neurons were voltage-clamped at −70 mV. The recording pipettes (3–5 MΩ) were filled with a solution containing (in mM) 124 K-gluconate, 5 NaCl, 1 $MgCl_2$, 0.2 EGTA, 10 HEPES, 2 MgATP, 0.1 Na_3GTP, and 10 phosphocreatine disodium (adjusted to pH 7.2 with KOH). Picrotoxin (100 μM) was invariably used to block $GABA_A$ receptor-mediated inhibitory synaptic currents in all experiments. The amplitudes of EPSCs were adjusted between 50 and 100 pA to obtain a baseline. Paired pulse stimulations with a 50-ms interpulse interval were given during the presynaptic-LTP recording. For presynaptic-LTP induction, 240 paired presynaptic stimuli (with 50-ms interpulse intervals) at 2 Hz were delivered to the presynaptic fibers at a holding potential of −70 mV. For postsynaptic-LTP induction, a pairing LTP protocol was used, by delivering 80 pulses at 2 Hz paired with postsynaptic depolarization at +30 mV. For 'no-pairing protocol' 80 pulses at 2 Hz without postsynaptic depolarization (Fig. 2A and B), and for 'depolarization-only group' postsynaptic depolarization at +30 mV without delivering pulses in presynaptic fibers were used (Fig. 2D). (Zhao et al., 2005). For miniature EPSC (mEPSC) recording, 0.5 μM tetrodotoxin was added in the perfusion solution. The initial access resistance was 15–30 MΩ, which was monitored throughout the experiment. Data were discarded if the access resistance changed >15% during the experiment. Data were filtered at 1 kHz and digitized at 10 kHz. Summary LTP graphs were constructed by normalizing data in 5-min epochs to the mean value of baseline EPSCs.

2.3. Behavior tests for fear conditioning

Mice were initially habituated to the conditioning cage, a mouse test cage (18 × 18 × 30 cm) with metal-grid floor connected to a shock generator (Med Associates, St. Albans, VT). The test cage was located inside a sound attenuated cabinet. Before each conditioning session, the test cage was wiped clean with 70% ethanol. During conditioning, the cabinet was illuminated and the behavior was captured with a monochrome CCD camera. The Video Freeze software (Med Associates) was used to control the delivery of both tones and foot shocks (Anagnostaras et al., 2010). For habituation on day1, five 4-kHz, 75-dB tones (conditioned stimulus), each of which was 30 s in duration, were delivered at variable intervals. During conditioning on day2, mice were subjected to five exposures of the conditioned stimulus (CS), each of which co-terminated with a 2-s, 0.75-mA foot shock (unconditioned stimulus, US), and were called the 'paired group'. And in Fig. 2H, we used CS/US paired group as control group. Mice that only received tone stimulus formed the 'CS-only group', and in the 'unpaired group', the CS did not co-terminate with an US. The test on day3 for fear memory was performed in a novel illuminated context in which mice were subjected to two exposures to an unreinforced CS (120-s inter-stimulus interval). The novel context was a cage with different dimensions (22 × 22 × 21 cm) and a floor texture

matching that of the conditioning cage. Prior to each use, the floor and walls of the novel cage were wiped clean with 0.5% acetic acid to make the scent distinct from that of the conditioning cage. Behavioral responses to the CS were recorded. Freezing behavior was analyzed with Video Freeze software. The electrophysiological experiments were performed immediately after conditioning.

A hot plate and the von Frey test were also used in addition to foot-shock to evaluate the effect of general thermal nociception- and mechanical nociception-induced pain and fear.

2.4. Behavior tests for anxiety-like behavior

In the elevated plus maze (EPM) test, mice were acclimatized to the room for 30 min before behavioral observation. The EPM (Med Associates) consisted of two open arms (250 lux) and two closed arms (35 lux) situated opposite of each other (Hogg, 1996). Animals were individually placed in the center square and allowed to move freely for 5 min. The number of entries and time spent in each arm were recorded.

To induce anxiety behavior, mice were subjected to a raised open arm for 5 min and used immediately for electrophysiology study. In addition, mice were placed in ventilated 50 mL Falcon tubes for 2 h per day (10:00–12:00 h) for 10 consecutive day to increase the baseline levels of anxiety.

In the open field test, mice were placed in an open field (43.2 × 43.2 × 30.5 cm; MED Associates) inside an isolation chamber with dim illumination and a fan. The Activity Monitor system (MED Associates) was used to record horizontal locomotor activity. This system utilizes paired sets of photo beams to detect movement. Each mouse was placed in the center of the open field, and activity was measured for 10 min.

2.5. Cannula implantation surgery and microinjection of drugs into the AIC

Mice were anesthetized by inhalation of isoflurane (1–3%). The head of each mouse was fixed into a stereotaxic frame, and an incision was made over the skull, exposing the surface. Two small holes were drilled above the AIC, and the dura was gently removed. Guide cannulas were placed 1.20 mm anterior to the bregma, 2.90 mm lateral to the midline, and 3.30 mm ventral to the surface of the skull over the AIC.

Microinjection was performed using a 35-gauge injector, 0.5 mm lower than the guide cannula. A motorized syringe pump (UMP3, WPI, USA) and a Hamilton syringe (Hamilton, Reno, NY, USA) were used for this experiment. An AAV construct with a fluorescent reporter (AAV-CMV-eGFP; Hanbio) was bilaterally injected (0.3 μl) to confirm the site in the AIC following sacrifice. UBP310 (0.1 μg) dissolved in sterile saline, or sterile saline alone as vehicle was delivered bilaterally into the AIC (0.5 μl/side over 5 min). The delivered volume was confirmed by observing the downward movement of the meniscus in calibrated polyethylene (PE10) tubing. The injector was left in place for 1 min to prevent any solution from flowing back up the guide. After microinjection, mice were returned to their home cages for 15 min, following which behavioral observations were recorded.

2.6. Tissue preparation, subcellular fractionation, and Western blot analysis

Subcellular fractionation was performed using a modified method (Berninghausen et al., 2007; Qiu et al., 2014) (see procedure, Fig. S3). The AIC region was dissected on ice in cold ACSF and homogenized in 0.32 M sucrose buffer [10 mM sucrose, 10 mM HEPES (pH 7.4)] containing a protease inhibitor cocktail and phosphatase inhibitor cocktail. The homogenates were centrifuged for 5 min at 2200 × *g* to yield P1 pellets and S1 supernatant. The supernatants were re-centrifuged for 20 min at 12,000 × *g*, yielding P2 pellets and S2 supernatant. To further digest synaptosomes and yield an insoluble "PSD-enriched" membrane fraction and a "non-PSD enriched" fraction, the P2 pellets were gently resuspended in 4 mM HEPES buffer [4 mM HEPES, 1 mM EDTA (pH 7.4)] and again centrifuged (12,000 × *g*, 20 min, 4 °C). Resuspension and centrifugation were repeated. The resulting pellet was resuspended in buffer A [20 mM HEPES, 100 mM NaCl, 0.5% Triton X-100 (pH 7.2)] and rotated slowly (15 min, 4 °C), followed by centrifugation (12,000 × *g*, 20 min, 4 °C). The supernatant S3 (Triton X-100–soluble NP fraction) containing non-PSD membranes was retained. The pellet P3 was resuspended in buffer B [20 mM HEPES, 0.15 mM NaCl, 1% TritonX-100, 1% deoxycholic acid, 1% sodium dodecyl sulfate (SDS), and 1 mM dithiothreitol (DTT), (pH 7.5), followed by gentle rotation (1 h, 4 °C) and centrifugation (10,000 × *g*, 15 min, 4 °C). The pellet P4 was discarded, and the supernatant S4 (Triton X-100-insoluble PSD fraction, postSM) was retained. The S3 was centrifuged at 50,000 × *g* for 30 min at 4 °C, yielding pellet P5 and supernatant S5.

Western blotting was conducted as described in previous studies (Shi et al., 2013). Protein concentrations were normalized with the Bradford assay. Electrophoresis of equal amounts of total protein was performed on SDS-polyacrylamide gels, and separated proteins were transferred onto polyvinylidene membranes at 4 °C. The membranes were blocked [2 h, room temperature, 5% milk or 5% bovine serum albumin (BSA) in TBST (tris-buffered saline with Tween 20 (TBST))] and incubated with primary antibodies (5% milk in TBST, 4 °C, overnight) [(1:1000 for SNAP-25 (Abcam, ab108990), 1:1000 for PSD-95 (Abcam, ab76115), 1:10000 for Synaptophysin (Abcam, ab32127), 1:500 for Gluk1 (Abcam, ab67316), and 1:500 for Gluk2 (Abcam, ab53092)]. Thereafter, the membranes were washed with TBST and incubated with the appropriate horseradish peroxidase (HRP)-coupled secondary antibody, followed by enhanced chemiluminescence detection.

2.7. Data analysis

Statistical comparisons were made using the unpaired or paired t-tests, one-way or two-way ANOVA, as appropriate. Significance between groups was tested with a Holm-Sidak or Tukey tests to adjust for multiple comparisons. For comparison of the LTP magnitude between different treatments, we compared the last 5 min of the recording with the first 5min of the baseline recording. All data were presented as the mean ± S.E.M. In all cases, $P < 0.05$ was considered statistically significant.

3. Results

3.1. Glutamate is the major excitatory synaptic transmitter in adult mouse AIC neurons

Whole-cell recordings were performed to determine the functional role of LTP in visually identified pyramidal neurons, in layers II and III of the AIC, and a bipolar stimulation electrode was placed in layer V/VI (Fig. 1A). The cells were classified as principal neurons on the basis of spike frequency adaptation in response to prolonged depolarizing current injection (Fig. 1B) (Tsvetkov et al., 2002). The neurons that received pure monosynaptic input were recorded by delivering 10 stimulation pulses at 20 Hz (holding at −70 mV; Fig. 1C), and it was found that these could be repetitively stimulated without failure (Fig. 1C). To test whether excitatory synaptic transmission is mediated by glutamate, EPSC was induced by single-pulse stimulation in the presence of a $GABA_A$ antagonist, PTX

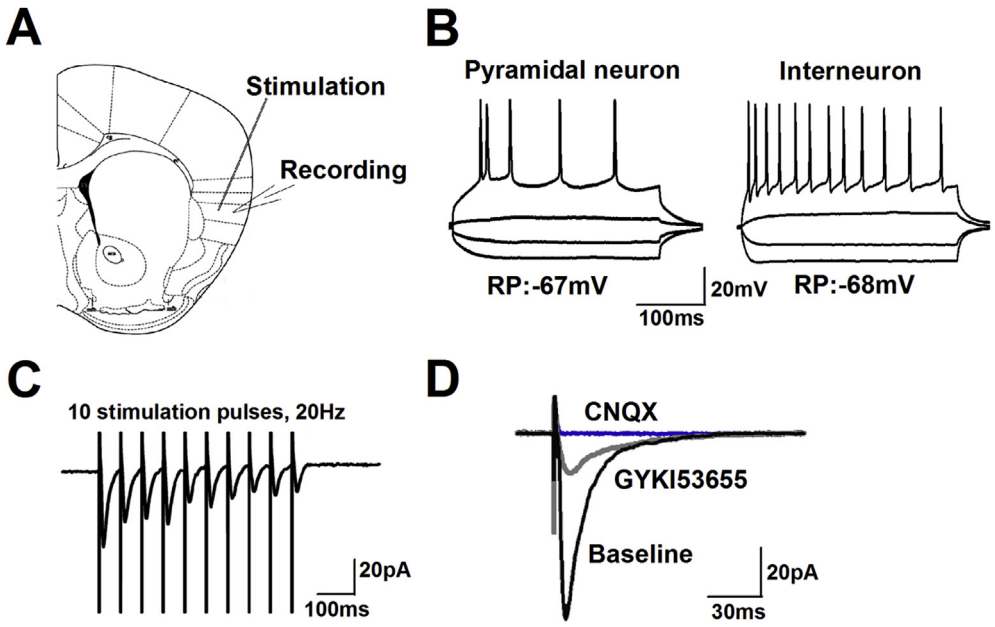

Fig. 1. Excitatory synaptic transmission in adult mouse AIC neurons. **(A)** Diagrams indicating placement of the stimulating and recording electrodes in the AIC. **(B)** When injected with current steps from −100 to 100 pA in 400 ms, pyramidal neurons fired repetitive action potentials with frequency adaptation (left). Interneurons showed fast-spike properties (right). RP: Resting Membrane Potential. **(C)** Monosynaptic input by 10 stimulation pulses at 20 Hz. **(D)** AMPA/KA EPSCs were recorded in the presence of PTX (100 μM) and AP-5 (50 μM) for 5 min, baseline (black trace). After the perfusion of GYKI53655 (100 μM) for 10 min (grey trace), a small residual current remained that could be totally blocked by CNQX (20 μM) (blue trace). (For interpretation of the references to colour in this figure legend, the reader is referred to the web version of this article.)

(100 μM), and a selective NMDAR antagonist AP-5 (50 μM). Then the neurons were subjected to a bath containing potent AMPA receptor antagonist GYKI53655 (100 μM); the remaining EPSCs were considered KAR-mediated (Fig. 1D). This KAR-mediated EPSC was completely blocked by bath application of an AMPA/KA receptor antagonist CNQX (20 μM; Fig. 1D).

Induced LTP requires postsynaptic NMDA receptors and fear conditioning occludes postsynaptic-LTP in the AIC.

To determine whether synaptic transmission undergoes LTP, synaptic stimulation was paired with postsynaptic depolarization (also referred to as "pairing training") (80 pulses of presynaptic stimulation at 2 Hz in layer V with postsynaptic depolarization at +30 mV) (Tsvetkov et al., 2004). This pairing training produced a significant, long-lasting potentiation of synaptic responses (mean = 158.0 ± 11.2% of baseline, n = 16; paired *t*-test, $p < 0.01$ versus baseline responses before the pairing training; Fig. 2A). In the control group, neurons were not subjected to pairing training, and synaptic responses were not significantly altered over the entire recording period (mean = 98.5 ± 4.6% of baseline response, n = 6; paired *t*-test, $p = 0.58$; Fig. 2B). Depolarization of the postsynaptic neuron to 30 mV without the 2-Hz presynaptic stimulation was not sufficient to induce LTP (mean = 98.1 ± 10.6% of baseline response, n = 7, paired *t*-test, $p = 0.66$, Fig. 2C), suggesting a possible role for pre-synaptically released glutamate in the induction process ().

To determine the source of enhanced intracellular Ca^{2+}, the role of NMDA-type glutamate receptors was examined in the AIC. These routes of Ca^{2+} delivery to the postsynaptic neuron are known to be important for synaptic plasticity in the insular cortex (Qiu et al., 2013). However, LTP was only partially blocked by AP-5, a competitive NMDA receptor antagonist (50 μM), with an average LTP of the EPSC being 131.2 ± 8% of the baseline value (n = 6, one-way ANOVA followed by LSD-*t* test, $F_{5,43} = 2.96$, $p < 0.05$, versus pairing training group, Fig. 2D&G). Consistent with the idea that a Ca^{2+} influx is required for LTP induction (Bolshakov and Siegelbaum, 1994), it was found that LTP was completely abolished by 10 mM BAPTA in the pipette solution (mean = 103.2 ± 11.3% versus pairing training group, n = 6, one-way ANOVA followed by LSD-*t* test, $F_{5,43} = 2.96$, $p < 0.01$, Fig. 2E&G), indicating that this LTP is dependent on the activation of NMDARs and elevated postsynaptic Ca^{2+} concentrations.

To study synaptic mechanisms of learned fear, a classic fear conditioning model was used (refer to Materials and Methods). It was found that pairing training protocol induced postsynaptic LTP in AIC synapses was significantly reduced in fear-conditioned animals immediately after day2 experiment (CS/US paired group, 126.8 ± 6.7%, n = 7, vs. pairing training group, 158.0 ± 11.2%, n = 16, one-way ANOVA followed by LSD-*t* test, $F_{5,43} = 2.96$, $p < 0.05$, Fig. 2F&G). The observed effect of the training procedure on LTP was specifically linked to fear conditioning, since LTP was not affected in mice that received CS only (151.8 ± 7.4%, $p = 0.65$, n = 6) or in CS/US unpaired control mouse (146.8 ± 11.4%, $p = 0.58$, n = 8). To directly address the role of NMDA receptor in fear memory acquisition in the AIC, we examined the effect NMDA blockade using MK-801. Microinjection of NMDA receptor antagonist MK-801 (2 μg in 0.5 μl per side) into the bilateral AIC before conditioning partially but significantly blocked mouse freezing behavior (MK-801, n = 11; vehicle, n = 10, t = 2.124, $p < 0.05$, unpaired *t*-test; Fig. 2H). In order to rule out any locomotor side effects, we tested locomotor activity in the open field after bilateral AIC microinjection of MK-801 (n = 5) or vehicle (n = 5). There was no difference in locomotor activity between groups when recorded 15 min or 1 day after injection. Taken together, this suggested that the NMDA receptor in the AIC is involved in the acquisition of fear memory.

3.2. Fear conditioning-induced LTP suggests a presynaptic mechanism

Both presynaptic and postsynaptic mechanisms have been suggested to contribute to LTP expression (Nicoll and Malenka, 1995). To determine whether presynaptic mechanisms are also involved in expression of LTP in the AIC, we measured paired-pulse

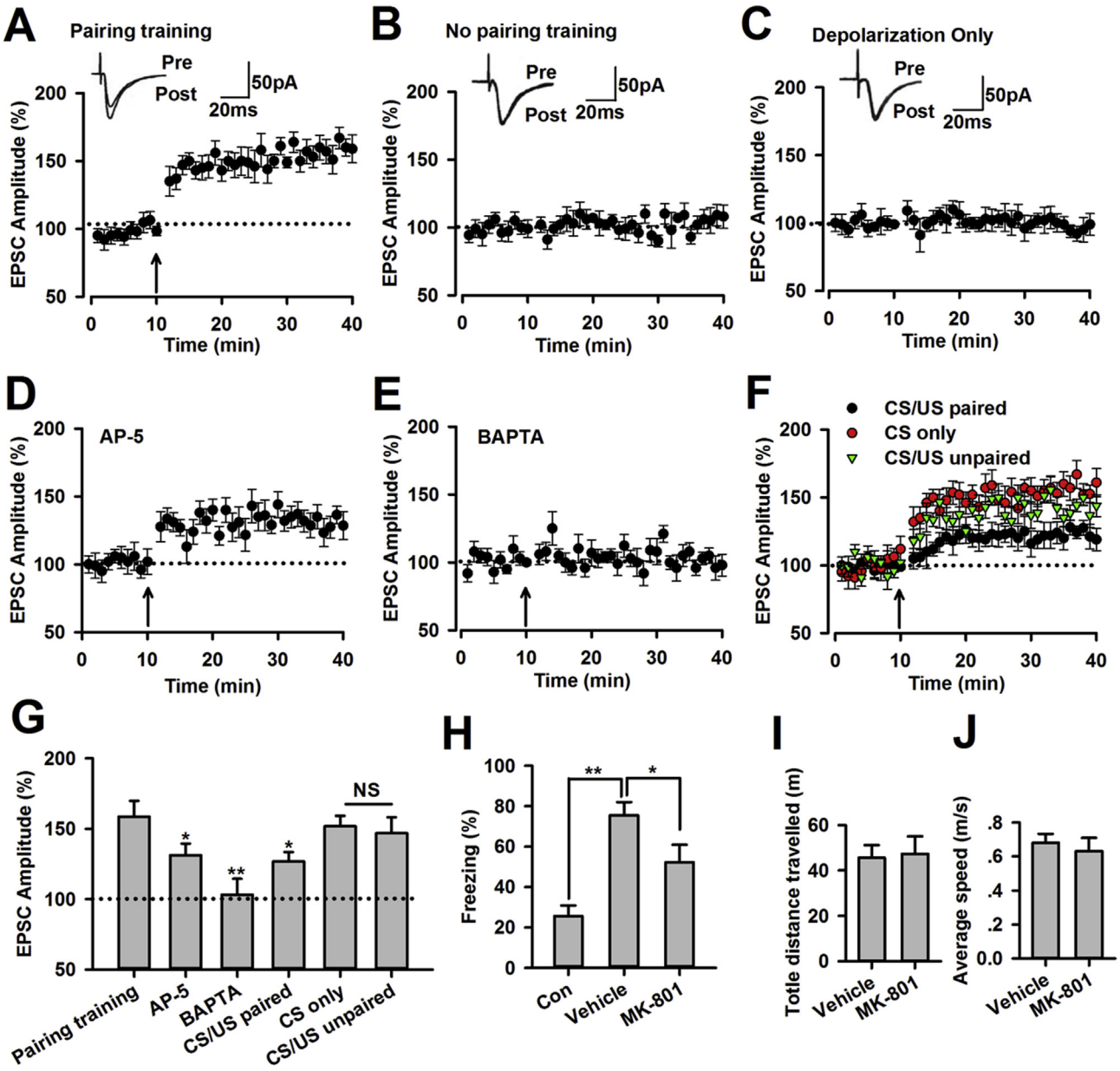

Fig. 2. Induction of LTP in the AIC synapses is postsynaptic and requires Ca^{2+} influx. **(A)** LTP was induced in pyramidal neurons (n = 16) in the adult AIC by the pairing training protocol (indicated by an arrow). The insets show averages of six EPSCs 5 min before and 25 min after the pairing training (arrow). The dashed line indicates the mean basal synaptic responses. **(B)** Basic synaptic transmission showing no change during recording without applying pairing training. The insets show averages of six EPSCs at the time points of 5 and 35min during the recording. **(C)** Depolarization of the postsynaptic neuron to 30 mV without the 2-Hz presynaptic stimulation was not sufficient to induce LTP (n = 6), suggesting a role for the presynaptically released glutamate in the induction process. The insets show averages of six EPSCs at the time points of 5 and 35min during the recording. **(D)** Effects of AP-5 on the pairing training-induced LTP. **(E)** LTP was completely blocked by application of BAPTA (n = 6) in the intracellular solution. **(F)** LTP recorded at the AIC synapses was occluded in fear-conditioned animals. (G) Summary of the effects of an NMDA receptor antagonist, postsynaptic injection of BAPTA, or conditioned fear on postsynaptic LTP. There was statistical difference when comparing control group (a pairing training LTP protocol) with AP-5, BAPTA or CS/US paired groups (one-way ANOVA, $F_{5,43} = 3.45$, $^{*}p > 0.05$). There was no difference comparing control group with CS only or CS/US unpaired groups (NS, $p > 0.05$). The mean amplitudes of EPSCs were determined at 35–40 min. Error bars represent SEM. **(H)** Pharmacological blockade of NMDAR in the AIC decreased fear behavior, $^{*}p < 0.05$. **(I, J)** Total distance travelled and average speed in the open field test was not significant different between these two groups.

facilitation (PPF), which is a phenomenon by which a second synaptic stimulation of equal magnitude evokes a larger synaptic response than the first and has been used as a tool to implicate presynaptic probability of transmitter release (Schulz et al., 1994), before and after fear conditioning. PPF was significantly decreased in AIC neurons after fear acquisition (Fear conditioning group, FC, n = 10) when compared with the control group (Con, n = 10; two-way repeated measures ANOVA, $F_{1,52=}9.63$, $p < 0.05$; Fig. 3A), indicating an increased presynaptic probability of transmitter release in AIC synapses. However, in the adjacent granular and dysagranular insula (GI/DI), the ratio of PPF did not differ between the FC (n = 8) and Con (n = 6) mice (two-way repeated measures ANOVA, $F_{1,26=}2.98$, $p = 0.62$, Fig. 3B). These results suggest that presynaptic transmission is selectively enhanced in the AIC of mice with fear conditioning.

Next, to investigate whether the reduced PPF observed in the synapses of the AIC might be associated with an increase of the release probability, we measured miniature EPSC, which revealed

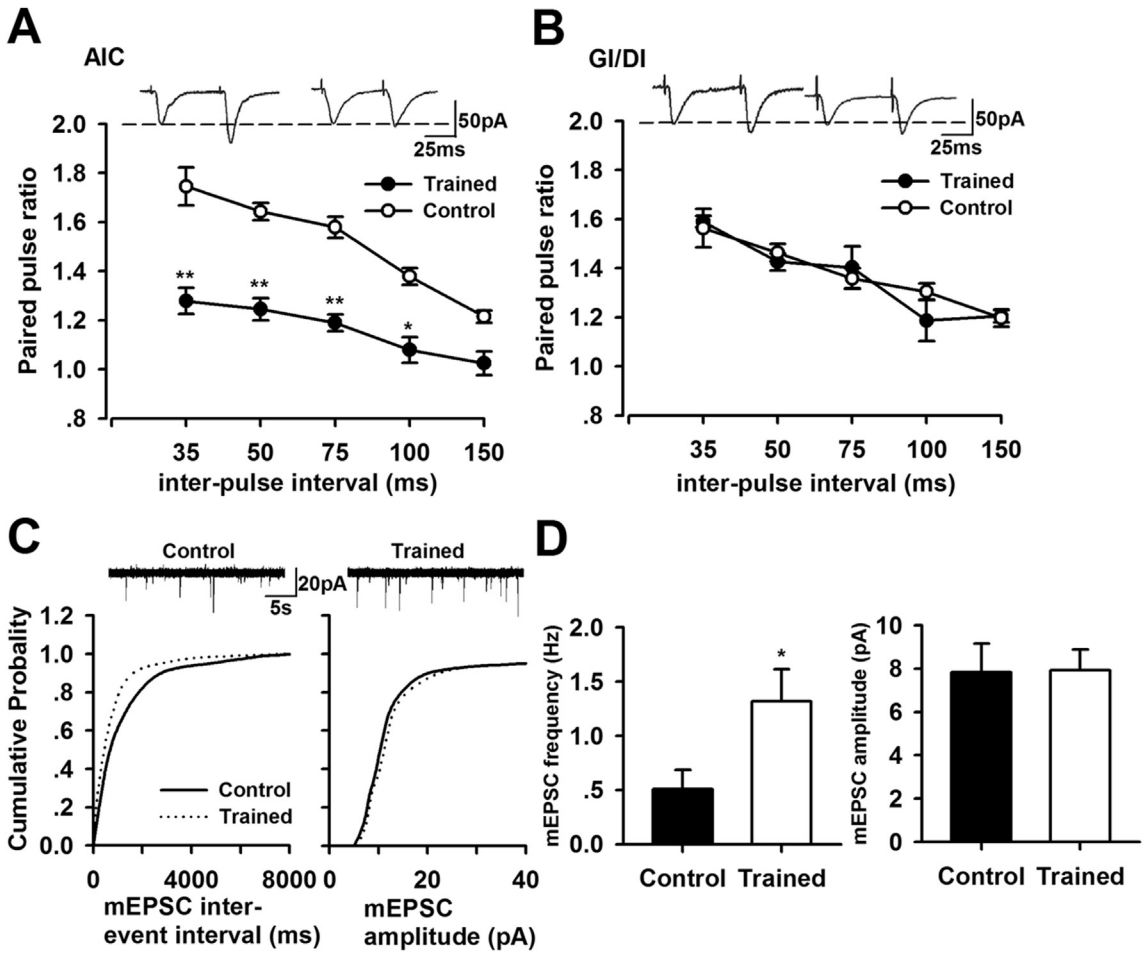

Fig. 3. LTP in the AIC is accompanied by an increase in neurotransmitter release. **(A)** The PPF (the ratio of EPSC2/EPSC1) was recorded at different inter-pulse intervals (IPIs: 35, 50, 75, 100, and 150 ms). Representative traces of the PPF with an interval of 50 ms recorded in the AIC. The PPF was significantly reduced at each interval in fear conditioning trained mice. Open circles, from control mice (Con), $n = 10$; filled circles, from fear conditioned mice (FC), n=17, two-way repeated measures ANOVA, $^{*}p<0.05$, $^{**}p<0.01$. **(B)** Representative traces of PPF at intervals of 50 ms recorded in the GI/DI show the PPF was not altered in either group of mice, n = 8. **(C)** Cumulative frequency (left) and amplitude (right) of the mEPSCs from the cells in Fig. 3A. Solid line, recording from a control mouse; dashed line, recording from a fear conditioned mouse. **(D)** mEPSC frequency (left) and amplitude (right) in neurons from control (n = 14) and fear conditioned (n = 11) mice, $^{*}p < 0.05$. Data are represented as mean ± SEM.

the quantal nature of presynaptic transmission. A significant increase in mEPSC frequency was detected in fear conditioned mice compared with controls (0.5 ± 0.02 Hz, n = 14; FC, 1.32 ± 0.29 Hz, n = 11; $p < 0.05$; Fig. 3 C, D), but there was no difference in the amplitude of mEPSCs between groups (Con, 7.84 ± 1.32 pA, n = 14; FC, 7.92 ± 0.95 pA, n = 11; $p < 0.05$; Fig. 3C and D). Together, these results indicate that enhanced synaptic transmission is attributable to an increase in the presynaptic probability of neurotransmitter release in AIC synapses of conditioned fear mice.

3.3. Induction of presynaptic-LTP is mediated by GluK1-containing KARs in AIC neurons

To investigate whether a presynaptic-LTP mechanism exists in AIC synapses, we employed a stimulation protocol that was successfully used previously to induce pre-LTP in the amygdala (Shin et al., 2010). After achieving a stable baseline recording in response to PPF (50-ms inter-pulse interval) for at least 10 min, we applied low-frequency stimulation (2 Hz for 2 min) at a holding potential of −70 mV in layer V/VI of the AIC in the presence of PTX (100 μM). This stimulation robustly increased the amplitude of evoked EPSCs in AIC neurons (161 ± 12.5% of baseline; Fig. 4A and B). In contrast, control neurons, which did not receive LTP induction, showed no change in the amplitude of EPSCs (102 ± 6.3%; Fig. 4A and B). The low-frequency stimulation and control groups were significantly different (one-way ANOVA, $F_{4,59} = 3.02$, $p < 0.05$, Fig. 4G). Meanwhile, the potentiation induced by the stimulation was associated with a reduction in the paired-pulse ratio (PPR; 85 ± 4% of baseline), which is commonly used as a measure of presynaptic function (Zucker and Regehr, 2002). In contrast, control neurons, which did not receive LTP induction, showed no change in the PPR (98 ± 4%). The low-frequency stimulation statistically altered the PPR (two-way ANOVA, $F_{1,64} = 6.98$, $p < 0.05$, Fig. 4C). Unlike conventional pairing-induced LTP (Tsvetkov et al., 2002), this form of synaptic potentiation was not blocked by the Ca^{2+} chelator (BAPTA, 20 mM) in the recording pipette solution, and therefore, it did not require postsynaptic Ca^{2+} influx for its induction (Fig. 4D). In addition, to determine whether presynaptic-LTP in the AIC is NMDAR dependent, we applied AP-5 in the bath solution. This presynaptic-LTP was not affected by the presence of AP-5 (Fig. 4E), indicating that AIC presynaptic-LTP is NMDAR independent and may require a presynaptic mechanism. However, this type of presynaptic-LTP could be blocked by bath application of a GluK1 receptor-specific antagonist, UBP310 (10 mM; 98 ± 10.2%, $p < 0.05$, UBP310 versus control presynaptic-LTP; Fig. 4F).

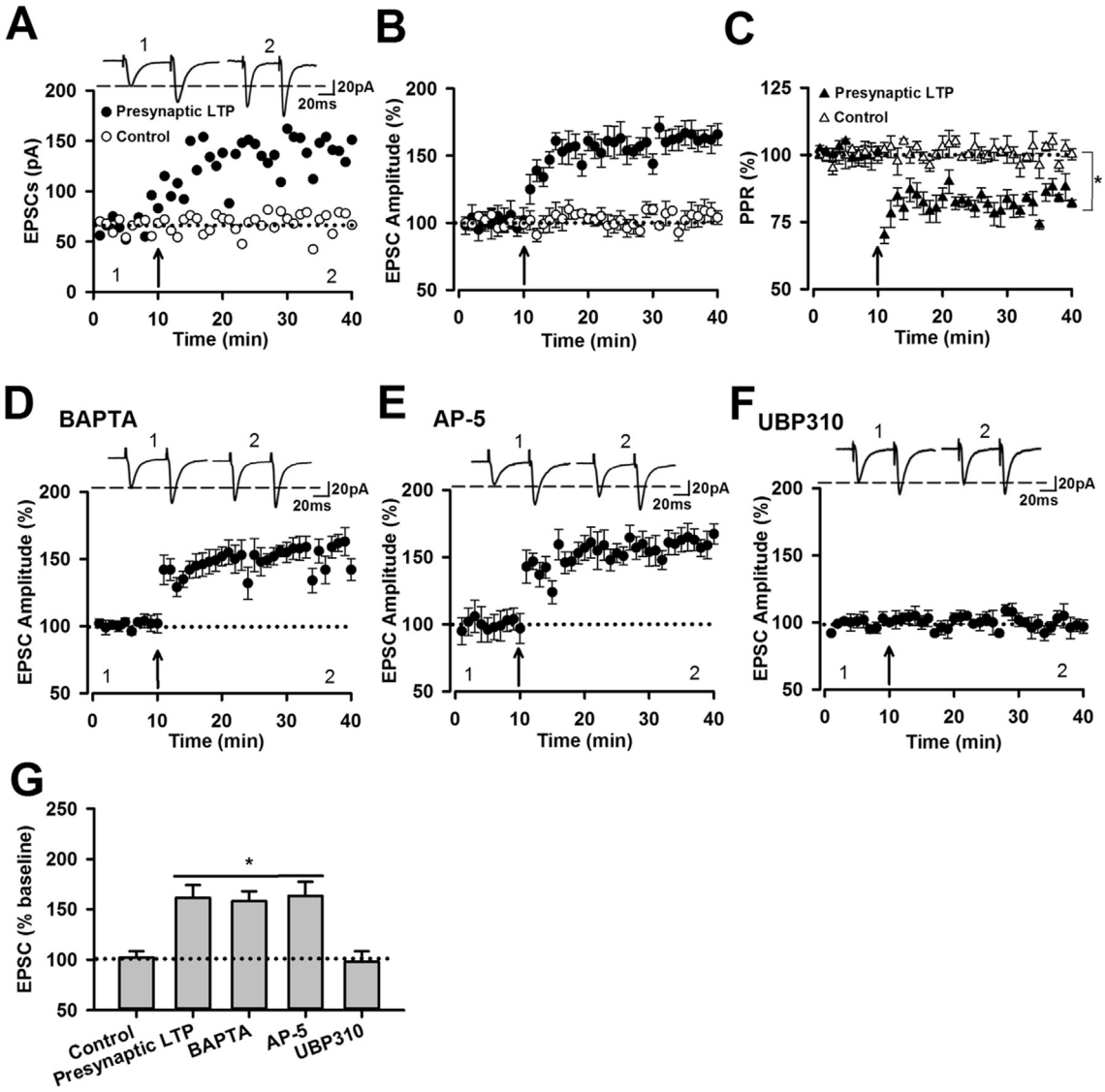

Fig. 4. Kainate receptors mediate the induction of presynaptic-LTP in the AIC. **(A)** Top: sample traces of EPSCs with paired-pulse stimulation at 50-ms inter-stimulus interval during baseline (1) and 40 min after presynaptic-LTP (2) at a holding membrane potential of −70 mV. Middle: a time course plot of a representative single example. The arrow indicates the time of LTP induction. **(B)** Pooled data from many neurons in many mice illustrating the time course of presynaptic LTP. presynapticLTP (filled circle, n = 20 neurons from 6 mice) and control (open circle, n = 13 neurons from 5 mice). **(C)** The PPR change estimated at 10-min intervals from baseline to 20 and 30 min after the induction stimulus, $^{*}p < 0.05$. **(D)** BAPTA (20 mM) in the recording pipette did not block pre-LTP (n = 11/8). **(E)** An NMDA receptor antagonist, AP-5 (50 mM), did not affect pre-LTP (n = 12/9). **(F)** A specific GluK1 antagonist, UBP310 (10 mM), completely blocked pre-LTP (n = 8/6). (G) Summary of the effects of postsynaptic injection of BATPA, an NMDA receptor antagonist, or a GluK1 antagonist on presynaptic LTP. There was statistical difference when comparing control with presynaptic LTP, AP-5, BAPTA, or UBP310 groups (one-way ANOVA, $F_{4,59} = 3.02$, $^{*}p < 0.05$). There was no difference comparing presynaptic LTP with AP-5, BAPTA, or UBP310 (NS, $p > 0.05$). The mean amplitudes of eEPSCs were determined at 35–40 min. Error bars represent SEM.

To further investigate possible mechanisms mediating cortical presynaptic-LTP, we studied the involvement of voltage-gated calcium channels (VGCCs), which are well known to regulate neurotransmitter release and contribute to presynaptic-LTP in other brain areas (Lauri et al., 2003; Fourcaudot et al., 2009). Bath application of an L-VGCC inhibitor, nimodipine (10 μM), had no effect on basal synaptic transmission (99.3 ± 6.1% of baseline, n = 8 neurons, paired *t*-test, $p < 0.05$; Fig. S1A). Next, we studied whether nimodipine could affect the induction and maintenance of presynaptic-LTP. Delivery of low-frequency stimulation in the presence of nimodipine failed to induce presynaptic-LTP (100.3 ± 5.4% of baseline, n = 6 neurons/5 mice, paired *t*-test, $p < 0.05$, Fig. S1B). However, induced presynaptic-LTP was insensitive to nimodipine when given 15 min after stimulation (142.8 ± 8.3% of baseline, n = 8 neurons/6 mice, paired *t*-test, $p < 0.05$, Fig. S1B). Bath application of GluK1-containing kainate receptor agonist (ATPA, 1 μM) could also induce a LTP-like phenomenon (147% ± 13% at 40min, one-way ANOVA, $F_{1,19} = 5.18$, $p < 0.05$; Fig. S1C). These findings indicate that L-VGCC coupled with GluK1-receptor activation is required for the induction but not maintenance of presynaptic-LTP in the AIC.

3.4. Fear conditioning and anxiety reduces presynaptic-LTP

Having established the existence of presynaptic-LTP in the AIC, we investigated the functional significance of this form of long-term synaptic plasticity. Therefore, we decided to determine whether presynaptic-LTP may be involved in the mediation of

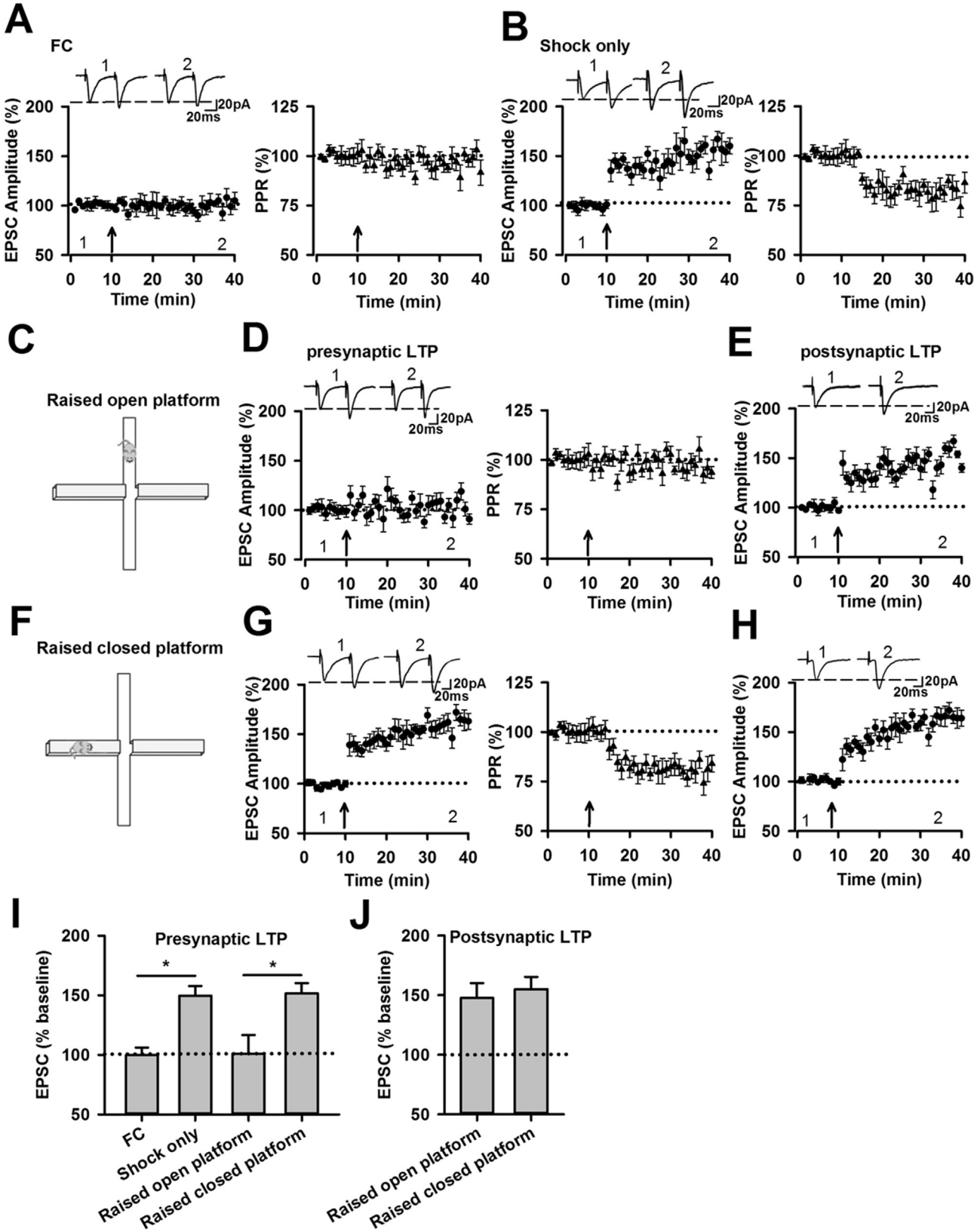

Fig. 5. Loss of presynaptic-LTP in fear and anxiety models. **(A)** Mice exposed to fear conditioning did not immediately exhibit presynaptic-LTP (left panel) and PPR (right panel) (n = 10/10). Sample traces of eEPSCs before (1) and 30 min after (2) the induction stimulus. **(B)** The shock only group showed normal presynaptic-LTP (left panel) and PPR (right panel) in the AIC. **(C)** Schematic diagram of raised open platform. **(D)** Mice exposed to the raised open platform blocking the closed arm did not exhibit presynaptic-LTP (left panel) and PPR (right panel) in the AIC (middle, n = 14). **(E)** Postsynaptic-LTP in the AIC was normal in mice exposed to the raised open platform (right, n = 10/9). Sample traces indicate EPSCs at baseline (1) and 30 min after the presynaptic-LTP induction protocol (2). Sample traces show eEPSCs at baseline (1) and 30 min after the pairing protocol (2). **(F)** Schematic diagram of raised closed platform. **(G)** Mice exposed to the raised closed platform blocking the open arm exhibit presynaptic-LTP in the AIC (middle, n = 12/10). **(H)** Postsynaptic-LTP in the AIC was normal in mice exposed to the raised closed platform (right, n = 10/8). Sample traces indicate EPSCs at baseline (1) and 30 min after the pre-LTP induction protocol (2). Sample traces show eEPSCs at baseline (1) and 30 min after the pairing protocol (2). **(I)** Summary of presynaotic-LTP experiments in fear conditioning, shock only raised open and closed platform models. **(J)** Summary of postsynaotic-LTP experiments in raised open and closed platform models.

emotive stimuli in the fear conditioning model. We found that the presynaptic-LTP was blocked by fear conditioning in the AIC of mice (99.8 ± 6.1%, one-way ANOVA, $F_{3,42} = 3.83$, $p < 0.05$; Fig. 5A&I). Moreover, PPR was also affected in response to the fear conditioning (98 ± 4% of baseline, Fig. 5A, right). Fear conditioning models usually employ an aversive US such as foot shock. This kind of acute pain can also cause an LTP-like phenomenon (Zhuo, 2014). Next, we tested whether foot shock alone could alter presynaptic-LTP. We found that it resulted in normal presynaptic-LTP (149.6 ± 8.2%, Fig. 5B) and the potentiation induced by the stimulation was also associated with a reduction in the PPR (83% ± 4% of baseline; Fig. 5B, right). Similarly, mice exposed to a hot plate or subjected to a von Frey test also showed normal presynaptic-LTP (hotplate; 153 ± 12.5%, von Frey; 162 ± 22.1%, Fig. S2C). We presumed that presynaptic-LTP is mainly related to enhance emotional salience processing in the AIC. Therefore, we exposed the mice in a raised open platform (blocking the closed arm) for 5 min, which is thought to increase the anxiety state of mice in this paradigm. After the exposure, presynaptic-LTP was found to be completely absent (101 ± 15%, n = 8 neurons/8mice, one-way ANOVA, $F_{3,42} = 3.83$, $p < 0.05$; Fig. 5D&I). The change of PPR was also abolished (Fig. 5D, right). Moreover, to test whether emotion processing is selective for presynaptic-LTP, we also examined postsynaptic-LTP in the mice that were exposed to the raised open platform. We found that a pairing protocol could lead to normal postsynaptic-LTP (147.1 ± 12.3%, n = 6 neurons/6mice, *t*-test, $p < 0.05$; Fig. 5E&J). In contrast mice exposed in the closed platform with the blocked open arm for 5 min showed normal presynaptic-LTP (151.3 ± 8.4%, n = 8 neurons/8 mice, one-way ANOVA, $F_{3,42} = 3.83$, $p < 0.05$; Fig. 5G&I) and postsynaptic-LTP (155.1 ± 15.6%, n = 6 neurons/6 mice, *t*-test, $p < 0.05$; Fig. 5H&J). Taken together, these results indicate that presynaptic-LTP is a potential mechanism for anxiety-like behavior.

3.5. Increased amount of presynaptic Gluk1 subunits in the AIC after fear conditioning

To assess whether presynaptic KARs are involved in anxiety-like behavior, we performed biochemical analyses to investigate the abundance of KAR subunits in different subcellular fractions. The synaptosome was separated and isolated into the pre- and post-synaptic membranes fraction using a modified method (Berninghausen et al., 2007) (see Experimental Procedures, Fig. S3). A clear separation of presynaptic membranes, postsynaptic membranes, synaptic vesicles, and cytosolic proteins was achieved as demonstrated by the distribution of SNAP-25, PSD-95, and Synaptophysin. KAR GluK1 subtype was located at both the pre- and post-synaptic fractions (Fig. 6A). We found that the abundance of presynaptic GluK1 was significantly increased immediately after fear conditioning (131 ± 5%, one-way ANOVA, $F_{2,20} = 6.28$, $p < 0.01$, n = 7 mice for each group; Fig. 6B, D). In contrast, no upregulation of post-synaptic GluK1 and pre- and post-synaptic GluK2 was observed after fear conditioning (n = 7 mice/group; Fig. 6B, D). Mice showed increased presynaptic GluK1 receptor expression after open arm exposure (124 ± 6%, one-way ANOVA, $F_{2,23} = 5.89$, $p < 0.01$, n = 8 mice/group; Fig. 6C, E). No effects on GluK1 and GluK2 expression were found in either the control or closed arm-exposed mice (Fig. 6C, E). Together, these data indicate that the synaptic GluK1 subunit is specifically increased in the AIC during fear and anxiety.

3.6. Effects of inhibiting GluK1-containing KARs in the AIC on fear and anxiety

The above results showed that expression and synaptic localization of KARs were enhanced in the insular cortex after fear and anxiety, which suggested that KARs in the insular cortex might contribute to fear- or anxiety-induced behavioral abnormalities in mice. To test this notion, we microinjected the Gluk1-specific antagonist UBP310 bilaterally into the AIC and evaluated changes in animal behavior (Fig. 7A). Microinjection of UBP310 (2 μg in 0.5 μl per side) bilaterally in the AIC before conditioning produced a significant reduction in freezing (UBP310, n = 10; vehicle, n = 10, one-way ANOVA, $F_{3,39} = 5.25$, $p < 0.01$; Fig. 7B). Moreover, in order to observe the combined effect of presynaptic and postsynaptic LTP on freezing, we blocked both mechanisms in the AIC and observed no additive effect on the animals' freezing behavior. In order to rule out any locomotor side effects, we tested locomotor activity in the open field after bilateral AIC microinjection. There was no difference in locomotor activity between the groups when recorded 15 min after injection (Fig. 7B). Next, to investigate the functional role of the AIC in anxiety, we used the elevated-plus maze (EPM), in which mice with anxiety symptoms spend less time in the open arms of the EPM (Carola et al., 2002). Mice were restrained in a 50 mL Falcon tubes before behavioral manipulations. Mice of the control group not restrained in high-stress environment spent more time in the open arm (Control group, 35.6 ± 3.3s, vs. Stress group, 10.2 ± 4.1s, n = 8 for each group, one-way ANOVA, $F_{3,31} = 4.86$, $p < 0.01$; Fig. 7C). Microinjection of UBP310 in the AIC increased open-arm time (24.6 ± 4.1s compared with Stress group, one-way ANOVA, $F_{3,31} = 4.86$, n = 8, $p < 0.05$; Fig. 7C). In addition, microinjection of ATPA (5 μg in 0.5 μl per side) in the AIC induced anxiety-like behavior (12.6 ± 6.3s compared with Control group, one-way ANOVA, $F_{3,31} = 4.86$, n = 8, $p < 0.01$; Fig. 7C)Taken together, these results suggest that the activation of Gluk1 in the AIC is important for the acquisition of fear and anxiety.

4. Discussion

In this study, it has been shown that pre- and post-synaptic mechanisms coexist during fear conditioning in the AIC. We believe that a form of presynaptic-LTP, related to abnormal salience stimuli processing, is expressed, and it involves GluK1-containing KARs and requires L-VGCC for induction. It was found that exposure to an elevated open platform without any US occludes presynaptic-LTP in the AIC. Furthermore, blocking insular GluK1-containing KARs reduced fear and anxiety behavior. Collectively, these data suggest that presynaptic-LTP at AIC synapses signals an anxious state that enhances the behavioral response to external environment stimuli.

4.1. Role of the AIC in fear and anxiety

Salience network abnormalities are prominent in mood and anxiety disorders. The AIC, as a key node of salience network, receives information about the salience stimulus (both appetitive and aversive) and relative value of the stimulus environment and integrates this information with the effects that these stimuli may have on the state of the body (Singer et al., 2009). Persistent dysphoric emotions such as fear are common DSM-5 symptoms of anxiety. Theories about fear have been dominated by the amygdala's contribution (Davis et al., 2010), but the amygdala does not solely account for fear or anxiety. There is accumulating evidence of altered insular functioning in patients with anxiety disorders, including panic disorder (Malizia et al., 1998), social phobia (Lorberbaum et al., 2004), generalized anxiety disorder (GAD) (Hoehn-Saric et al., 2004), obsessive-compulsive disorder (OCD) (Mataix-Cols et al., 2004), and PTSD (Weston, 2014). Anxiety-prone individuals have bilaterally increased insular activation during the processing of emotions (Stein et al., 2007). Inhibition or lesion of

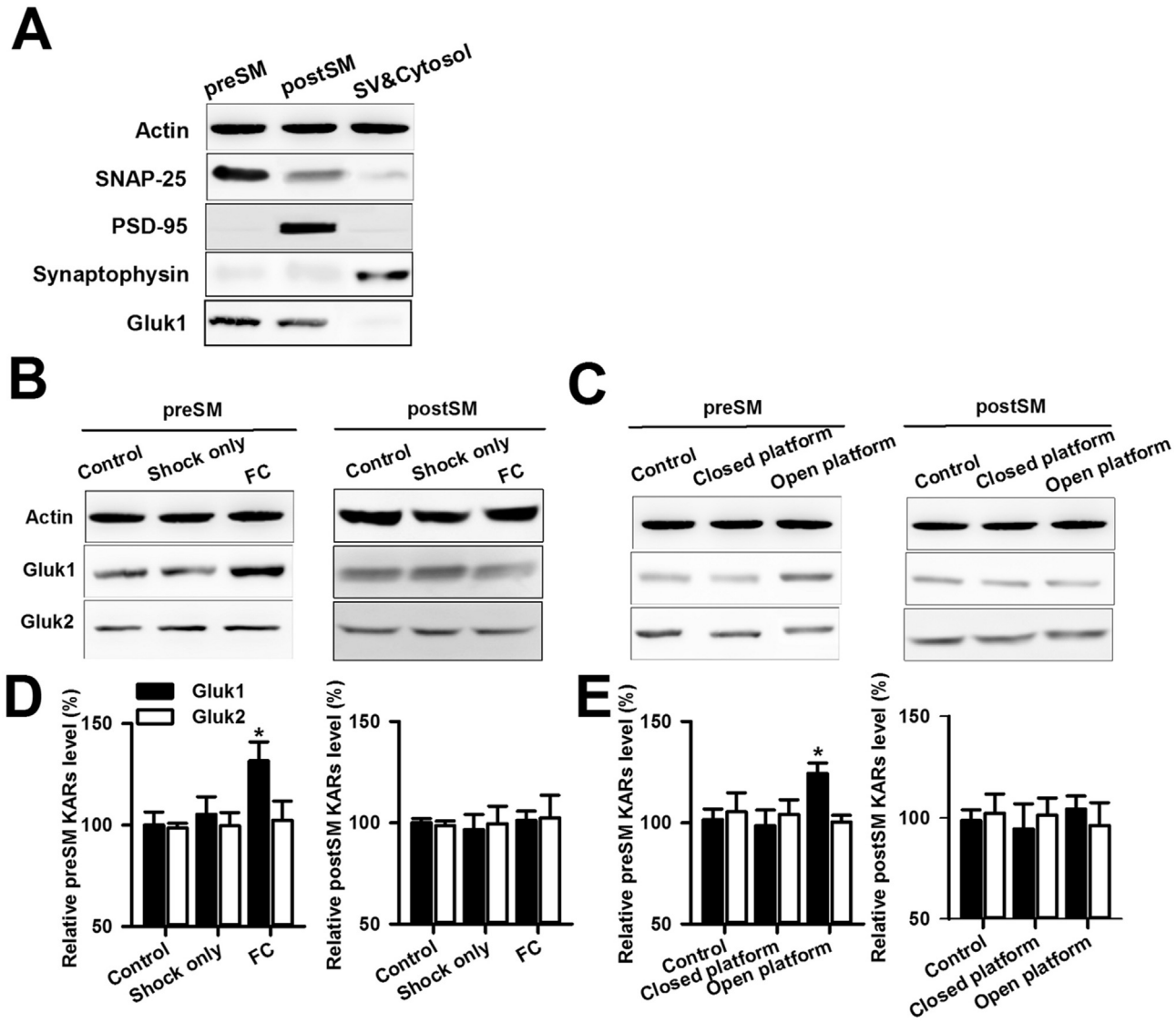

Fig. 6. Presynaptic GluK1, but not GluK2, is upregulated in the AIC after fear and anxiety. **(A)** Fractionation of the insular cortex was probed for SNAP-25, PSD-95, synaptophysin, and Gluk1 to confirm the accuracy of the subcellular fractionation procedure. **(B)** Representative Western blots for GluK1 and GluK2 in the presynaptic membrane (preSM) and postsynaptic membrane (postSM) fractions of the AIC obtained from the control, shock only, and fear conditioning trained group. **(C)** Representative Western blots for GluK1 and GluK2 in the presynaptic and postsynaptic membranes of control, raised closed platform, and open platform groups. **(D)** The abundance of GluK1 in the preSM fraction was significantly increased upon fear exposure (n = 6 mice for each group). The abundance of GluK1 in the postSM fraction showed no changes after fear conditioning (n = 7 mice for each group). **(E)** The abundance of GluK1 in the preSM fraction was significantly increased in the raised open platform group, but not raised after closed platform exposure (n = 7 mice for each group). The abundance of GluK1 in the postSM fraction showed no changes between raised closed and open platform (n = 7 mice for each group).

the insular cortex induces attenuated sensitivity to the emotions (Terasawa et al., 2015). However, whether synaptic transmission in the AIC undergoes plastic changes during emotional processing needs to be explored further. In this study, a classic fear conditioning model was used to investigate the function of the AIC in aversive stimulus processing. Our data indicate that fear conditioning is accompanied by an occlusion of postsynaptic-LTP, is mediated by postsynaptic NMDARs, and coexists with long-term enhancement in neurotransmitter release through a presynaptic-LTP mechanism.

4.2. KARs mediate presynaptic-LTP in the AIC

KARs are tetrameric combinations of multiple subunits, namely GluK1, GluK2, GluK3, GluK4, and GluK5. With the molecular identification of KAR subunits, the functional description of KARs within the central nervous system is much clearer (Lerma and Marques, 2013). Although originally described as being postsynaptic, accumulating evidence indicates that KARs are located in significant numbers in presynaptic terminals where they modulate neurotransmitter release (Jane et al., 2009; Huettner, 2003). Abnormalities in glutamatergic neurotransmission are considered to be an important factor contributing to mental disorders. In the insular cortex, KARs mediate excitatory synaptic transmissions (Koga et al., 2012), and our previous work has shown that LTP can be induced in the adult mouse insular cortex (Liu et al., 2013). In the present study, freezing behavior was accompanied by occlusion of the PPF ratio and an increase in mEPSC frequency after fear conditioning. To determine whether it coexists with presynaptic-LTP, a well-described protocol was used in other limbic brain regions, such as hippocampus and amygdala (Shin et al., 2010; Zalutsky and Nicoll, 1990). GluK1-containing KARs, but not NMDARs, seem to be

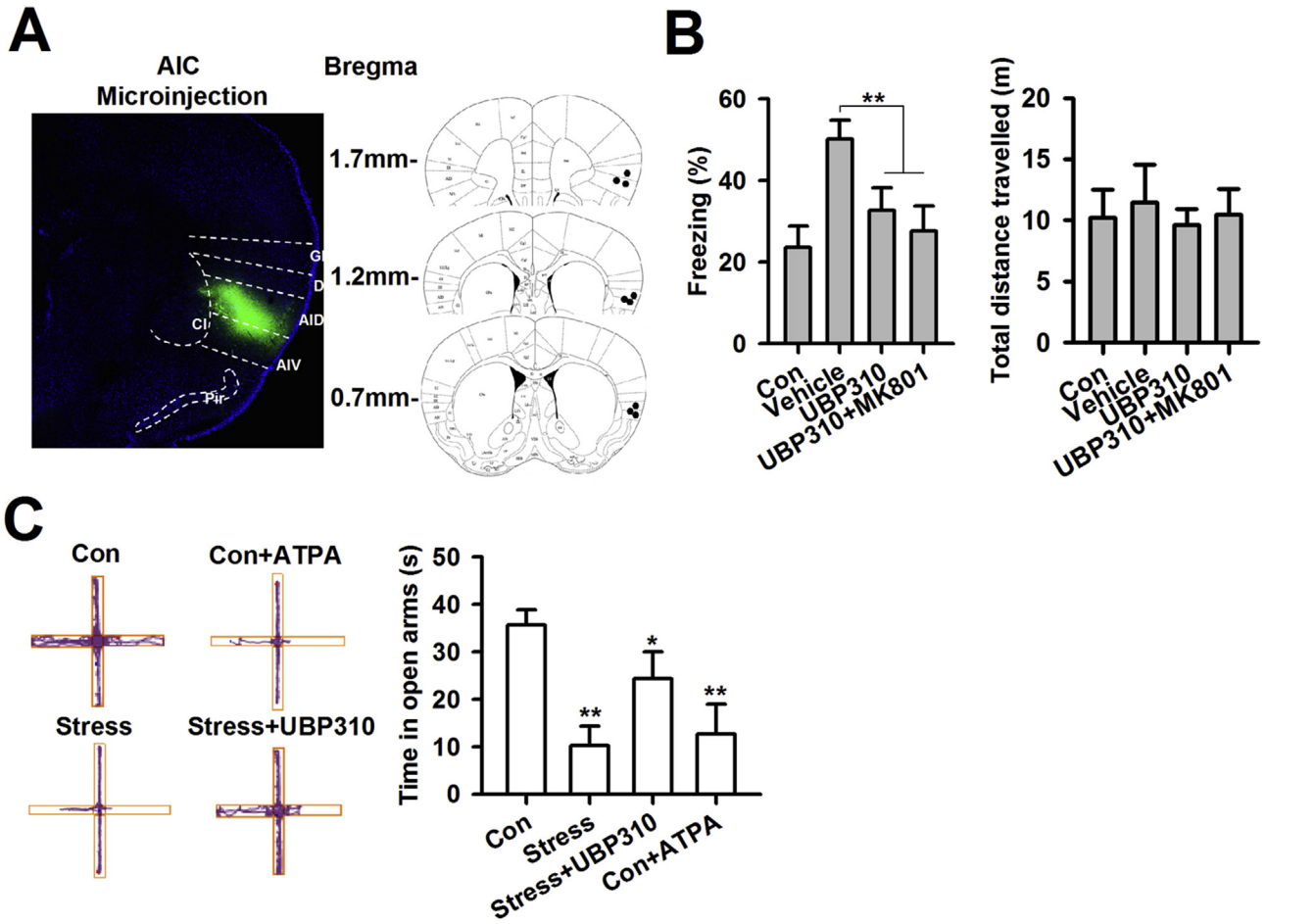

Fig. 7. Effect of Gluk1 blockade on learned fear and anxiety. **(A)** Representative coronal section (left) showing injection sites using AAV-CMV-eGFP for the AIC. Scale bar, 1 mm. The right column shows the cannula tip placements in mice injected with the GluK1-KAR antagonist UBP310 (black circles in the AIC, n = 9). **(B)** Pharmacological blockade of GluK1 or both GluK1 and NMDA receptors in the AIC decreased fear behavior and had no effect on mice locomotion, n = 10 each group, $^{**}p < 0.01$. **(C)** Pharmacological blockade of GluK1 in the AIC decreased anxiety-like behavior in EPM, and using KAR agonist could induce anxiety-like behavior in EPM, n = 8, $^{*}p < 0.01$.

sufficient for induction of presynaptic-LTP in the AIC. Although postsynaptic application of BAPTA did not affect presynaptic-LTP, application of nimodipine in the bath solution could block this form of LTP, indicating that presynaptic calcium influx is required for induction of presynaptic-LTP. These findings show that the GluK1 subunit plays an important role in mediating presynaptic neurotransmitter release.

4.3. Synaptic plasticity mechanism for fear and anxiety in the AIC

Fear is elicited upon factual, acute sensory input, whereas anxiety can be evoked by potential, circumstantial, and anticipated threats (Grupe and Nitschke, 2013; Tye et al., 2011). However, the brain areas and neuromodulator systems that contribute to fear and anxiety exhibit immense overlap. LTP is one form of synaptic plasticity that has been widely studied in emotional memory (Bliss and Collingridge, 1993). Much research has focused on the discovery of the contribution of neuronal and synaptic plasticity mechanisms within the brain regions to fear and anxiety (Tye et al., 2011; Adhikari et al., 2015). The insular cortex, especially the anterior agranular part, has a strong connection with the amygdala (Reep and Winans, 1982). In this study, we found that fear conditioning not only occluded postsynaptic-LTP by a pairing training protocol, but also increased presynaptic neurotransmitter release and blocked presynaptic-LTP. Although foot shock alone had little effect on pre-LTP induction, a raised open platform test was employed to investigate the effects of emotional factors on synaptic plasticity. As discussed above, emotional stimuli only (mice explored the open arm without any physical stimulation) can cause long-term presynaptic neurotransmitter release. This could explain why clinical patients with anxiety disorders, because they have hyper-plasticity, exhibit increased attentive and over-prepared behavior in the face of an unpredictable threat.

4.4. Involvement of presynaptic KARs in fear and anxiety

KARs containing the GluK1 subunit have an impact on both excitatory and inhibitory neurotransmission in brain regions such as the amygdala and hippocampus, which have been found to play potential roles in the regulation of mood disorders (Sihra et al., 2014). Although KARs act as key players in the regulation of synaptic network activity, many properties and functions of these proteins remain elusive. The precise pre-, extra-, and post-synaptic localization of KARs plays a critical role in neuronal functions. In this study, increased presynaptic neurotransmitter release was found to be mainly mediated by the presynaptic membrane Gluk1 receptor resulting in fear and anxiety-like behaviour. Trafficking of KARs has been reviewed recently (Pahl et al., 2014). As a next step, experiments are needed to determine the signaling pathway by which KARs activity is regulated. However, this study does provide

evidence that presynaptic GluK1 plays a role in fear and anxiety via pharmacological methods. However, cell-specific studies need to be carried out to eliminate the confounding effects of pharmacological agents over both pre- and post-synaptic structures.

In conclusion, we have identified a presynaptic form of LTP that coexists with a postsynaptic form of LTP in AIC synapses. Abolishing presynaptic-LTP with the Gluk1 antagonist UBP310 is associated with an anxiolytic effect. Presynaptic-LTP mediates an emotional signal in the AIC salience network. Thus, presynaptic-LTP in ALC projecting neurons could be a potential synaptic plasticity mechanism for fear and anxiety.

These experiments, along with further studies, will help reveal the participation of KARs in negative emotional behavior and whether they would be suitable targets for therapeutic interventions for anxiety disorders.

Funding and disclosure

The authors declare no conflict of interest.

Acknowledgments

This work was supported by the Natural Science Foundation of Beijing (Grant No. 7154229) and National Natural Science Foundation of China (Grant No. 81402912).

Appendix A. Supplementary data

Supplementary data related to this article can be found at https://doi.org/10.1016/j.neuropharm.2017.10.037.

References

Adhikari, A., et al., 2015. Basomedial amygdala mediates top-down control of anxiety and fear. Nature 527 (7577), 179–185.
Alves, F.H., et al., 2013. Involvement of the insular cortex in the consolidation and expression of contextual fear conditioning. Eur. J. Neurosci. 38 (2), 2300–2307.
Anagnostaras, S.G., et al., 2010. Automated assessment of pavlovian conditioned freezing and shock reactivity in mice using the video freeze system. Front. Behav. Neurosci. 4.
Berninghausen, O., et al., 2007. Neurexin Ibeta and neuroligin are localized on opposite membranes in mature central synapses. J. Neurochem. 103 (5), 1855–1863.
Bliss, T.V., Collingridge, G.L., 1993. A synaptic model of memory: long-term potentiation in the hippocampus. Nature 361 (6407), 31–39.
Bliss, T.V., Collingridge, G.L., 2013. Expression of NMDA receptor-dependent LTP in the hippocampus: bridging the divide. Mol. Brain 6, 5.
Bolshakov, V.Y., Siegelbaum, S.A., 1994. Postsynaptic induction and presynaptic expression of hippocampal long-term depression. Science 264 (5162), 1148–1152.
Bortolotto, Z.A., et al., 1999. Kainate receptors are involved in synaptic plasticity. Nature 402 (6759), 297–301.
Carola, V., et al., 2002. Evaluation of the elevated plus-maze and open-field tests for the assessment of anxiety-related behaviour in inbred mice. Behav. Brain Res. 134 (1–2), 49–57.
Craig, A.D., 2002. How do you feel? Interoception: the sense of the physiological condition of the body. Nat. Rev. Neurosci. 3 (8), 655–666.
Craig, A.D., 2009. How do you feel–now? The anterior insula and human awareness. Nat. Rev. Neurosci. 10 (1), 59–70.
Davis, M., et al., 2010. Phasic vs sustained fear in rats and humans: role of the extended amygdala in fear vs anxiety. Neuropsychopharmacology 35 (1), 105–135.
Etkin, A., Wager, T.D., 2007. Functional neuroimaging of anxiety: a meta-analysis of emotional processing in PTSD, social anxiety disorder, and specific phobia. Am. J. Psychiatry 164 (10), 1476–1488.
Fourcaudot, E., et al., 2009. L-type voltage-dependent Ca(2+) channels mediate expression of presynaptic LTP in amygdala. Nat. Neurosci. 12 (9), 1093–1095.
Gilmartin, M.R., Balderston, N.L., Helmstetter, F.J., 2014. Prefrontal cortical regulation of fear learning. Trends Neurosci. 37 (8), 455–464.
Grupe, D.W., Nitschke, J.B., 2013. Uncertainty and anticipation in anxiety: an integrated neurobiological and psychological perspective. Nat. Rev. Neurosci. 14 (7), 488–501.
Hoehn-Saric, R., Schlund, M.W., Wong, S.H., 2004. Effects of citalopram on worry and brain activation in patients with generalized anxiety disorder. Psychiatry Res. 131 (1), 11–21.
Hogg, S., 1996. A review of the validity and variability of the elevated plus-maze as an animal model of anxiety. Pharmacol. Biochem. Behav. 54 (1), 21–30.
Huettner, J.E., 2003. Kainate receptors and synaptic transmission. Prog. Neurobiol. 70 (5), 387–407.
Jane, D.E., Lodge, D., Collingridge, G.L., 2009. Kainate receptors: pharmacology, function and therapeutic potential. Neuropharmacology 56 (1), 90–113.
Jaskolski, F., Coussen, F., Mulle, C., 2005. Subcellular localization and trafficking of kainate receptors. Trends Pharmacol. Sci. 26 (1), 20–26.
Ko, S., et al., 2005. Altered behavioral responses to noxious stimuli and fear in glutamate receptor 5 (GluR5)- or GluR6-deficient mice. J. Neurosci. 25 (4), 977–984.
Koga, K., et al., 2012. Kainate receptor-mediated synaptic transmissions in the adult rodent insular cortex. J. Neurophysiol. 108 (7), 1988–1998.
Lauri, S.E., et al., 2003. A role for Ca^{2+} stores in kainate receptor-dependent synaptic facilitation and LTP at mossy fiber synapses in the hippocampus. Neuron 39 (2), 327–341.
LeDoux, J.E., 2000. Emotion circuits in the brain. Annu. Rev. Neurosci. 23, 155–184.
LeDoux, J., 2012. Rethinking the emotional brain. Neuron 73 (4), 653–676.
Lerma, J., 2003. Roles and rules of kainate receptors in synaptic transmission. Nat. Rev. Neurosci. 4 (6), 481–495.
Lerma, J., Marques, J.M., 2013. Kainate receptors in health and disease. Neuron 80 (2), 292–311.
Liu, M.G., et al., 2013. Long-term potentiation of synaptic transmission in the adult mouse insular cortex: multielectrode array recordings. J. Neurophysiol. 110 (2), 505–521.
Lorberbaum, J.P., et al., 2004. Neural correlates of speech anticipatory anxiety in generalized social phobia. Neuroreport 15 (18), 2701–2705.
Malizia, A.L., et al., 1998. Decreased brain GABA(A)-benzodiazepine receptor binding in panic disorder: preliminary results from a quantitative PET study. Arch. Gen. Psychiatry 55 (8), 715–720.
Mataix-Cols, D., et al., 2004. Distinct neural correlates of washing, checking, and hoarding symptom dimensions in obsessive-compulsive disorder. Arch. Gen. Psychiatry 61 (6), 564–576.
Nicoll, R.A., Malenka, R.C., 1995. Contrasting properties of two forms of long-term potentiation in the hippocampus. Nature 377 (6545), 115–118.
Nicoll, R.A., Schmitz, D., 2005. Synaptic plasticity at hippocampal mossy fibre synapses. Nat. Rev. Neurosci. 6 (11), 863–876.
Nistico, R., et al., 2011. Synergistic interactions between kainate and mGlu receptors regulate bouton Ca signalling and mossy fibre LTP. Sci. Rep. 1, 103.
Pahl, S., et al., 2014. Trafficking of kainate receptors. Membr. (Basel) 4 (3), 565–595.
Paulus, M.P., Stein, M.B., 2006. An insular view of anxiety. Biol. Psychiatry 60 (4), 383–387.
Paxinos, G., Franklin, K.B.J., 2001. The Mouse Brain in Stereotaxic Coordinates, second ed. Academic Press, , San Diego.
Peterson, A., et al., 2014. Resting-state neuroimaging studies: a new way of identifying differences and similarities among the anxiety disorders? Can. J. Psychiatry 59 (6), 294–300.
Qiu, S., et al., 2013. An increase in synaptic NMDA receptors in the insular cortex contributes to neuropathic pain. Sci. Signal 6 (275), ra34.
Qiu, S., et al., 2014. GluA1 phosphorylation contributes to postsynaptic amplification of neuropathic pain in the insular cortex. J. Neurosci. 34 (40), 13505–13515.
Reep, R.L., Winans, S.S., 1982. Afferent connections of dorsal and ventral agranular insular cortex in the hamster Mesocricetus auratus. Neuroscience 7 (5), 1265–1288.
Rogan, M.T., Staubli, U.V., LeDoux, J.E., 1997. Fear conditioning induces associative long-term potentiation in the amygdala. Nature 390 (6660), 604–607.
Rumpel, S., et al., 2005. Postsynaptic receptor trafficking underlying a form of associative learning. Science 308 (5718), 83–88.
Saper, C.B., 1982. Convergence of autonomic and limbic connections in the insular cortex of the rat. J. Comp. Neurol. 210 (2), 163–173.
Schulz, P.E., Cook, E.P., Johnston, D., 1994. Changes in paired-pulse facilitation suggest presynaptic involvement in long-term potentiation. J. Neurosci. 14 (9), 5325–5337.
Seeley, W.W., et al., 2007. Dissociable intrinsic connectivity networks for salience processing and executive control. J. Neurosci. 27 (9), 2349–2356.
Shi, C.J., Cassell, M.D., 1998. Cortical, thalamic, and amygdaloid connections of the anterior and posterior insular cortices. J. Comp. Neurol. 399 (4), 440–468.
Shi, T.Y., et al., 2013. A new chiral pyrrolyl alpha-nitronyl nitroxide radical attenuates beta-amyloid deposition and rescues memory deficits in a mouse model of Alzheimer disease. Neurotherapeutics 10 (2), 340–353.
Shin, L.M., Liberzon, I., 2010. The neurocircuitry of fear, stress, and anxiety disorders. Neuropsychopharmacology 35 (1), 169–191.
Shin, R.M., et al., 2010. Hierarchical order of coexisting pre- and postsynaptic forms of long-term potentiation at synapses in amygdala. Proc. Natl. Acad. Sci. U. S. A. 107 (44), 19073–19078.
Shin, R.M., Higuchi, M., Suhara, T., 2013. Nitric oxide signaling exerts bidirectional effects on plasticity inductions in amygdala. PLoS One 8 (9), e74668.
Sihra, T.S., Flores, G., Rodriguez-Moreno, A., 2014. Kainate receptors: multiple roles in neuronal plasticity. Neuroscientist 20 (1), 29–43.
Singer, T., Critchley, H.D., Preuschoff, K., 2009. A common role of insula in feelings, empathy and uncertainty. Trends Cogn. Sci. 13 (8), 334–340.
Stein, M.B., et al., 2007. Increased amygdala and insula activation during emotion processing in anxiety-prone subjects. Am. J. Psychiatry 164 (2), 318–327.
Terasawa, Y., et al., 2015. Attenuated sensitivity to the emotions of others by insular lesion. Front. Psychol. 6, 1314.

Tsvetkov, E., et al., 2002. Fear conditioning occludes LTP-induced presynaptic enhancement of synaptic transmission in the cortical pathway to the lateral amygdala. Neuron 34 (2), 289–300.
Tsvetkov, E., Shin, R.M., Bolshakov, V.Y., 2004. Glutamate uptake determines pathway specificity of long-term potentiation in the neural circuitry of fear conditioning. Neuron 41 (1), 139–151.
Tye, K.M., et al., 2011. Amygdala circuitry mediating reversible and bidirectional control of anxiety. Nature 471 (7338), 358–362.
Uddin, L.Q., 2015. Salience processing and insular cortical function and dysfunction. Nat. Rev. Neurosci. 16 (1), 55–61.
Wendt, J., et al., 2008. Brain activation and defensive response mobilization during sustained exposure to phobia-related and other affective pictures in spider phobia. Psychophysiology 45 (2), 205–215.
Weston, C.S., 2014. Posttraumatic stress disorder: a theoretical model of the hyperarousal subtype. Front. Psychiatry 5, 37.
Wu, L.J., et al., 2007. Increased anxiety-like behavior and enhanced synaptic efficacy in the amygdala of GluR5 knockout mice. PLoS One 2 (1), e167.
Xu, H., et al., 2008. Presynaptic and postsynaptic amplifications of neuropathic pain in the anterior cingulate cortex. J. Neurosci. 28 (29), 7445–7453.
Zalutsky, R.A., Nicoll, R.A., 1990. Comparison of two forms of long-term potentiation in single hippocampal neurons. Science 248 (4963), 1619–1624.
Zhao, M.G., et al., 2005. Deficits in trace fear memory and long-term potentiation in a mouse model for fragile X syndrome. J. Neurosci. 25 (32), 7385–7392.
Zhuo, M., 2014. Long-term potentiation in the anterior cingulate cortex and chronic pain. Philos. Trans. R. Soc. Lond B Biol. Sci. 369 (1633), 20130146.
Zucker, R.S., Regehr, W.G., 2002. Short-term synaptic plasticity. Annu. Rev. Physiol. 64, 355–405.